Science & Technology Development Journal 2024, 27(1):3308-3314

Open Access Full Text Article

Engineering and Technology: Research article

Controlling the absorption region of multi-shaped silver nanoparticles for SERS applications

Le Ngoc Thu Nguyen[1,2], Hoai Nhan Luong[1,2], Ngoc Bao Tri Pham[1,2], Le Thai Duy[1,2], Cong Khanh Tran[1,2], Ngoc Phuong Nguyen[3,4], Vinh Quang Dang[1,2,*]

[1]*Faculty of Materials Science and Technology, University of Science, 227 Nguyen Van Cu Street, District 5, Ho Chi Minh City 700000, Vietnam*

[2]*Vietnam National University, Ho Chi Minh City (VNU-HCM) 700000, Vietnam*

[3]*Institute of Applied Materials Science, Vietnam Academy of Science and Technology (VAST), 29TL Street, Thanh Loc Ward, District 12, Ho Chi Minh City, Vietnam*

[4]*Graduate University of Science and Technology, VAST, Hoang Quoc Viet Street, Cau Giay, Ha Noi, Vietnam*

Correspondence

Vinh Quang Dang, Faculty of Materials Science and Technology, University of Science, 227 Nguyen Van Cu Street, District 5, Ho Chi Minh City 700000, Vietnam

Vietnam National University, Ho Chi Minh City (VNU-HCM) 700000, Vietnam

Email: vinhquangntmk@gmail.com

History

- Received: 2024-01-09
- Accepted: 2024-02-18
- Published Online: 2024-3-31

DOI :

https://doi.org/10.32508/stdj.v27i1.4238

Check for updates

ABSTRACT

Introduction: Silver nanoparticles (Ag NPs) are pivotal in advancing surface-enhanced Raman scattering (SERS) due to their exceptional plasmonic properties. Yet, conventional synthesis methods often fail to precisely control their shape and size, impacting SERS efficiency. This study introduces a novel synthesis approach using hydrogen peroxide (H2O2) to tailor Ag NP morphologies, aiming to optimize their plasmonic resonance for improved SERS detection of hazardous substances. **Methods:** We utilized a chemical reduction process with H2O2 to etch and shape Ag NPs, adjusting H2O2 concentrations to control nanoparticle morphology. The characterization of the nanoparticles involved SEM, TEM, and XRD for morphology and structure, with UV-Vis spectroscopy determining their absorption spectra. **Results:** The approach yielded Ag NPs with variable shapes and absorption wavelengths (330 nm to 740 nm), directly correlating H2O2 concentration with morphological changes. SEM and TEM showed diverse nanoparticle shapes, and XRD confirmed their crystalline structure. Notably, nanoparticles tuned to specific absorption wavelengths significantly enhanced SERS detection of Rhodamine B. **Conclusion:** Our method effectively produces multi-shaped Ag NPs with tunable optical properties, enhancing SERS application in detecting trace organic compounds. This streamlined synthesis process offers new possibilities for environmental monitoring and safety assessments.

Key words: Multi-shaped silver nanoparticles, SERS, Rhodamine B, plasmon resonance

INTRODUCTION

Over the decades, nanomaterials have played a crucial role in various scientific fields, contributing significantly to technological advancements and industrial applications [1–3]. The synthesis of nanoparticles using various noble metals has attracted considerable research interest due to their unique properties and potential applications in optoelectronics, catalysis, antibacterial agents, bio-sensors, and surface-enhanced Raman scattering (SERS) [4–7]. Among metal nanoparticles, such as Pd, Cu, Au, Zn, Sn, Co, etc., silver nanoparticles (Ag NPs) have particularly attracted researchers' attention due to their excellent electrical conductivity and strong plasmonic characteristics [8]. Numerous studies have shown that the properties of silver nanoparticles depend on their shape, size, size distribution, and crystal structure. For instance, rice-shaped silver nanoparticles exhibit two absorption peaks in the visible and near-infrared regions [9], while spherical silver nanoparticles typically show absorption peaks in the near-ultraviolet region [10]. Additionally, UV-Vis analysis reveals that small silver nanoparticles have high optical absorption and exhibit a redshift [11,12]. Consequently, extensive research has been conducted to synthesize silver nanoparticles with controllable morphology and distribution. Various techniques, including chemical methods, microwave techniques, and biological synthesis, have been employed to synthesize silver nanoparticles with diverse shapes, such as spheres, rods, wires, sheets, cubes, and arrays [13–20]. These methods each have their own advantages for specific synthesis purposes. However, they also face significant limitations, such as low reaction efficiency, time consumption, expensive and complex equipment, and difficulties in size control [21]. Thus, chemical reduction methods are widely used for synthesizing silver nanoparticles across various fields, including food technology, cosmetics, medical and dental diagnostics, especially in the detection and degradation of harmful organic substances [21–24]. For example, a research group led by Jagpreet Singh used Trigonella foenum-graecum (TF) leaf extract as a reducing agent to synthesize silver nanoparticles for photocatalytic degradation applications [25]. In 2017, Mutasem M. Al-Shalalfeh and colleagues used sodium borohydride as a stabilizing and reducing agent to synthesize spherical silver nanoparticles for SERS substrate applications in de-

Cite this article : Nguyen L N T, Luong H N, Pham N B T, Duy L T, Tran C K, Nguyen N P, Dang V Q. **Controlling the absorption region of multi-shaped silver nanoparticles for SERS applications**. *Sci. Tech. Dev. J.* 2024; 27(1):3308-3314.

tecting ketoconazole in agricultural products[26]. Additionally, Al-Shalalfeh's team fabricated two types of silver nanoparticles using sodium borohydride and trisodium citrate dehydrate, aiming to use them as SERS substrates for detecting 2-thiouracil. The average sizes of these silver nanoparticles were approximately 15 nm and 60 nm, with peak absorption around 400 - 430 nm[27]. In the VNUHCM Journal of Science and Technology Development, Nguyen Tran Gia Bao developed Ag NPs by reducing silver ions in AgNO3 using sodium borohydride or sodium citrate as reducing agents, along with surface-active agents like poly(vinyl alcohol) (PVA), poly(vinyl pyrrolidone) (PVP), and cetyltrimethylammonium bromide (CTAB). The synthesized AgNPs solution, with an absorption peak in the range of 410 - 450 nm, was employed for the detection of organic substances, including Crystal Violet (CV) and Rhodamine B (RhB), at a concentration of 10^-8M[28].

In general, the studies mentioned synthesize spherical-shaped silver nanoparticles (Ag NPs) with an absorption wavelength of around 400 nm. This characteristic limits their resonance with the excitation wavelengths of lasers commonly used in modern Raman spectroscopy devices (532 nm or 785 nm). Surface-enhanced Raman scattering (SERS) is significantly augmented by the unique nanostructure of noble metals, which can concentrate light through localized surface plasmon resonance (LSPR)[8]. The surface morphology of nanoparticles leads to varying surface plasmon resonances (SPR)[29], making it crucial to develop methods to shift the absorption wavelength to enhance SERS signals. Techniques to modify the absorption of Ag NPs include the electrochemical synthetic method[30], irradiation methods[31], and chemical reduction[32], among others. Yet, chemical synthesis, which involves modifying the shape of pre-formed nanoparticles, remains popular due to its straightforward experimental procedures, high efficiency, and suitability for large-scale production[21].

In this study, we synthesized diverse morphologies of silver nanoparticles (MAg NPs) in shapes such as triangular, hexagonal, and disc-shaped, adjusting the peak absorption wavelength between 330 nm and 740 nm by varying the concentration of the oxidizing agent hydrogen peroxide (H2O2). The shape transformation reaction involves reducing silver ions (Ag+) in a spherical silver solution using sodium borohydride (NaBH4) in the presence of H2O2 and citrate as a capping agent. Adjusting the H2O2 concentration allows for the development of silver nanoparticles with desired morphology and absorption wavelength to enhance Raman signals. Furthermore, we synthesized a SERS substrate using MAg NPs for detecting Rhodamine B (C28H31ClN2O3), an industrial dye often used in unauthorized food coloring, posing significant health risks. The Raman spectroscopy results demonstrate the substrate's effective detection of Rhodamine B (RhB), suggesting new research avenues in detecting harmful substances in food.

MATERIALS-METHODS

Chemical materials

Silver nitrate ($AgNO_3$) - 99% (Sigma-Aldrich), sodium citrate ($Na_3C_6H_5O_7$) - 99% (Sigma-Aldrich), sodium borohydrid ($NaBH_4$, 98,0%, Scharlau, Spain), hydroxyl peroxide (H_2O_2, 30%, Sigma-Aldrich).

Characteristics

Silver nanoparticles' size, morphology, and distribution were analyzed through scanning electron microscopy (SEM, Hitachi S-4800) and transmission electron microscopy (TEM, JEOL, JEM-1400). The crystal structure of MAg NPs were identified via X-ray diffraction (XRD) using a D8 Advance-Bruker diffractometer operating at 40 kV, 100 mA, with a Cu/Kα radiation source (λ = 0.154 nm). Raman spectra were recorded using a Raman spectrometer with an excitation source at 532 nm.

Fabrication processes

The synthesis process of MAg NPs includes two main steps: nucleation and fabrication of multi-shaped silver nanoparticles.

Step 1: Nucleation

Three beakers were simultaneously prepared, each containing a solution of silver nitrate ($AgNO_3$, 0.25 mM), sodium citrate ($Na_3C_6H_5O_7$, 0.25 mM), and sodium borohydride ($NaBH_4$, 10 mM), respectively. Subsequently, $AgNO_3$ and $Na_3C_6H_5O_7$ were stirred together at room temperature for 30 minutes. Next, $NaBH_4$ was slowly added to the mixture above, resulting in the formation of a germ solution (Figure 1a).

Step 2: Fabrication of multi-shaped silver nanoparticles

5ml H_2O_2, 0.02M $AgNO_3$ and 0.05287M $NaBH_4$ were added to the germ solution which was diluted with DI water (ratio 2:5). The resulting silver solution was then continuously stirred for 30 minutes to stabilize the MAg NPs (Figure 1b).

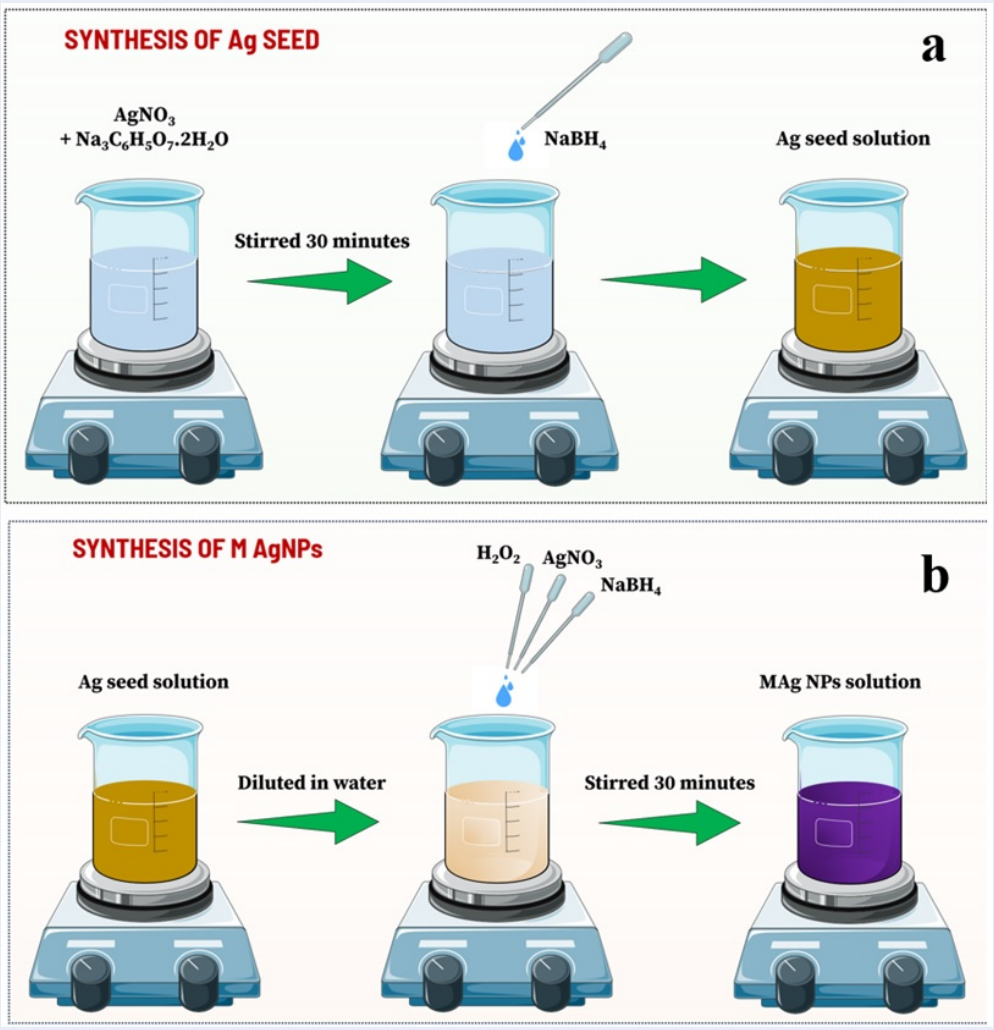

Figure 1: Synthesis process of **a)** germ solution and **b)** multi-shaped silver nanoparticles

RESULTS

The X-ray diffraction pattern of the multi-shaped silver nanoparticles that were synthesized according to the above process is presented in Figure 2b. The diffraction peaks at 2θ values with 27.81°, 32.16°, 38.12°, 46.21°, 54.83°, and 57.39°, correspond to the lattice surfaces (210), (122), (111), (231), (142), and (241) within the face-centered cubic (FCC) structure of pure silver (JCPDS, no. 04-0783)[33]. We synthesized multi-shaped silver solutions labeled as S0, S1, S2, S3, S4, corresponding to different concentrations of H_2O_2 at 0 %, 7 %, 8 %, 9 %, 10 %, respectively, to investigate the wavelength absorption changes. Also, the absorption spectra of five MAgNPs samples (Figure 2a) revealed peaks at 392 nm, 487 nm, 548 nm, 660 nm, and 738 nm.

The SEM and TEM images in Figure 3 depict the size and morphology outcomes of MAg NPs. The silver nanoparticle solution prepared exhibits various shapes, including triangles, hexagons, spheres, etc., ranging in size from 30 nm to 150 nm, with an average particle size of 38.641 nm.

The samples with distinct absorption peaks (487 nm, 548 nm, 660 nm, 738 nm) were employed as SERS substrates to explore their efficacy in detecting RhB at a concentration of 1 ppm (Figure 4a). The results reveal that all samples exhibit the capability to amplify Raman signals of RhB at 620, 1197, 1279, 1360, 1509, 1525, 1595, and 1645 cm^{-1} (Table 1).

An essential criterion for assessing the reliability of a SERS sample is the synchronization of Raman signals. As depicted in Figure 4b, the SERS signal was examined at random locations on sample S2 with a RhB

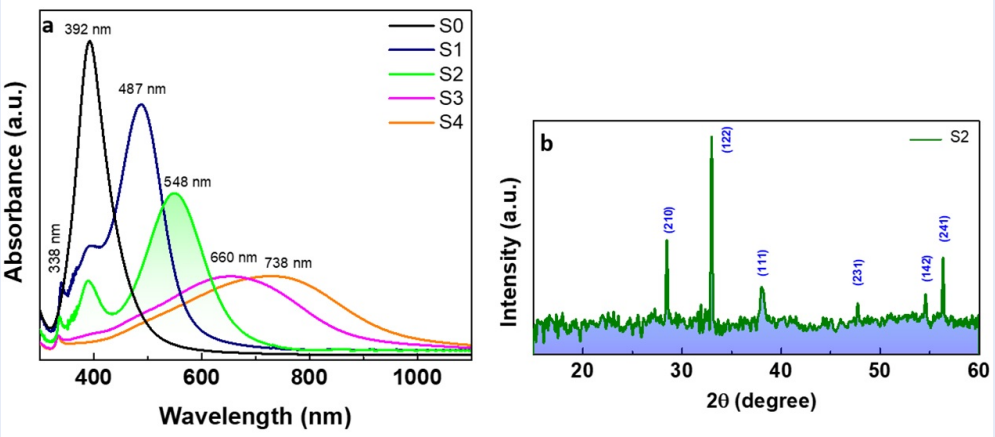

Figure 2: **a)** UV-Vis absorption spectra and **b**) XRD diffraction pattern of MAg NPs

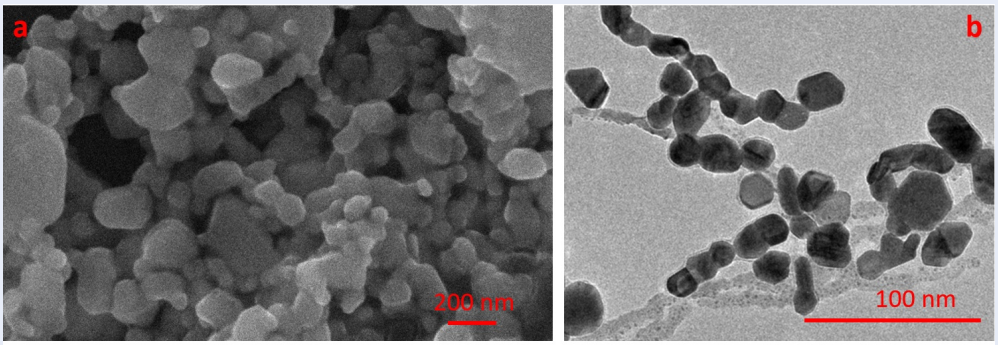

Figure 3: **a)** SEM images and **b)** TEM images of MAg NPs

Table 1: Band assignment of Rhodamine B [34,35]

Solid Raman	SERS	Vibrational Description
619 cm^{-1}	620 cm^{-1}	Aromatic bending
1195 cm^{-1}	1197 cm^{-1}	Aromatic C-H bending
1275 cm^{-1}	1279 cm^{-1}	C-C bridge-bands stretching
1356 cm^{-1}	1360 cm^{-1}	Aromatic C-C stretching
1506 cm^{-1}	1509 cm^{-1}	Aromatic C-C stretching
1525 cm^{-1}	1525 cm^{-1}	Aromatic C-C stretching
1595 cm^{-1}	1595 cm^{-1}	C=C stretching
1645 cm^{-1}	1645 cm^{-1}	Aromatic C=C stretching

concentration of 1 ppm.

DISCUSSION

In Figure 2b, the diffraction peaks corresponding to the crystallographic planes (210), (122), (111), (231), (142), and (241) of the face-centered cubic (FCC) structure of pure silver confirm the formation of silver crystals in the solution after the reaction. Furthermore, the UV-vis absorption spectra reveal the multimodal plasmon resonance oscillations of the MAg NPs. A distinct peak at 338 nm is attributed to the out-of-plane quadrupole plasmon resonance (OPQPR), while absorption bands at 487 nm, 548 nm, 660 nm, and 738 nm in the four MAg NP samples correspond to the in-plane dipole plasmon resonance (IPDPR) [36]. Additionally, an increase in H2O2 concentration leads to a redshift, suggesting oxidative corrosion of the initial silver seeds and a sub-

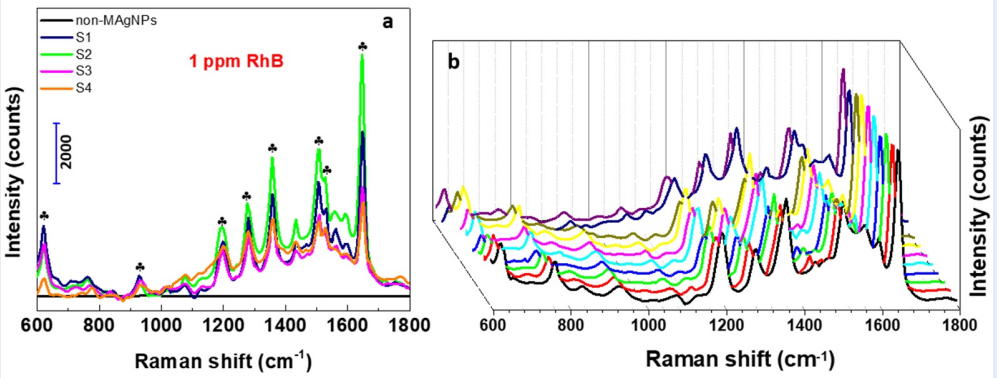

Figure 4: The Raman spectra of RhB (1 ppm) **a)** based on distinct SERS substrates, and **b)** at different locations on sample S2

sequent increase in size or edge length [10]. This observation underscores that silver nanoparticles, with their diverse morphologies, often exhibit more complex plasmon vibration modes than simple spheres, enabling control over the absorption wavelength by adjusting the H2O2 concentration. The size and morphological characteristics of the MAg NPs, as shown in Figure 3, also demonstrate the successful synthesis of multi-shaped silver nanostructures through the growth corrosion method. The investigation of the Rhodamine B (RhB) detection capability of the SERS substrate based on MAg NPs, presented in Figure 4a, clearly indicates that all samples enhance Raman signals through characteristic oscillations as detailed in Table 1. Notably, sample S2 shows the highest signal enhancement among the samples tested, attributed to its absorption wavelength of 548 nm effectively resonating with the excitation laser source's wavelength of 532 nm. Importantly, Figure 4b shows no significant disparity in the intensity of characteristic peaks in the Raman spectra at different locations, indicating that the synthesized samples possess practical consistency and high reliability.

The etching-growth process, which employs hydrogen peroxide (H2O2), was used to produce multi-shaped silver nanoparticles with the desired absorption wavelength. The synthesis procedure consists of two main stages: the corrosion stage and the growth stage. Importantly, the corrosion process is crucial in determining the final structure of the nanocrystals. It accomplishes this by either completely removing energetically unfavorable particles or by etching to form sharp corners and edges [37]. Hydrogen peroxide exhibits aspect-selective corrosive properties towards metallic silver species while also acting as a reducing agent for silver ionic species, as demonstrated by equations (1) to (5) [38–41].

H_2O_2 as an oxidizing agent:

$Ag^+ + e^- \rightarrow Ag$ ($E^0 = 0.7996$ V) (1)

$H_2O_2 + 2e^- \rightarrow 2HO^-$ ($E^0 = 0.867$ V) (2)

$2Ag + H_2O_2 \rightarrow Ag^+ + 2HO^-$ ($E^0 = 0.068$ V) (3)

H_2O_2 as an reducing agent:

$H_2O_2 + 2HO^- \rightarrow 2H_2O + O_2 + 2e^-$ ($E^0 = 0.146$ V) (4)

$H_2O_2 + 2Ag^+ + 2HO^- \rightarrow 2Ag + 2H_2O + O_2$ ($E^0 = 0.947$ V) (5)

During the growth period, $AgNO_3$ and $NaBH_4$ are introduced sequentially, resulting in the reduction of Ag^+ ions and the generation of MAg NPs, as illustrated by the following equation (6):

$2Ag^+ + 4BH_4^- + 7H_2O \rightarrow 2Ag^0 + B_4O_7^{2-} + 15H_2$ (6)

Due to its potent reducing capability, $NaBH_4$ rapidly reduces Ag^+ ions and facilitates the growth of symmetrical facets in MAg NPs and secondary seed particles [42]. Consequently, the resulting silver nano solution exhibits diverse morphologies, resulting in varying absorption wavelengths when altering the H_2O_2 concentration.

CONCLUSIONS

Multi-shaped silver nanoparticles were successfully synthesized, exhibiting absorption at distinct wavelengths (487, 548, 660, and 738 nm) through a rapid and straightforward process. Notably, among these nanoparticles, those with an absorption peak at 548 nm demonstrated superior enhancement of the Raman signal for Rhodamine B (RhB) at a concentration of 1 ppm. Furthermore, the corrosion-growth mechanism behind the formation of these nanoparticles has been elucidated. We anticipate that the findings from

this study will pave the way for the application of silver nanoparticles in various fields, especially in detecting low-concentration toxic organic compounds in the future.

COMPETING INTERESTS

The authors assert that there are no conflicts of interest related to the publication of this article.

AUTHORS' CONTRIBUTIONS

L. N. T. Nguyen: carried out the experiment, writing manuscript. **L. T. Duy**, **N. B. T. Pham**: measured and analyzed UV-Vis, XRD data. **L. N. T. Nguyen**, **C. K. Tran**: measured, analyzed SEM, TEM data. **N. P. Nguyen**, **H. N. Luong**: investigated SERS effect through measuring and analyzing Raman Spectra. **V. Q. Dang**: managed the experiment, collected data to write the paper.

ACKNOWLEDGMENTS

This research is funded by Vietnam National University, Ho Chi Minh City (VNU-HCM) under grant number B2023-18-14.

REFERENCES

1. Iravani S, Korbekandi H, Mirmohammadi SV, Zolfaghari B. Synthesis of silver nanoparticles: chemical, physical and biological methods. Res Pharm Sci 2014; 9: 385-406;.
2. Baig N, Kammakakam I, Falath W. Nanomaterials: a review of synthesis methods, properties, recent progress, and challenges. Materials Advances 2021; 2: 1821-1871;Available from: https://doi.org/10.1039/D0MA00807A.
3. Wu Q, Miao W, Zhang Y, Gao H, Hui D. Mechanical properties of nanomaterials: A review. Nanotechnology Reviews 2020; 9: 259-273;Available from: https://doi.org/10.1515/ntrev-2020-0021.
4. Keskenler EF, Tomakin M, Doğan S, Turgut G, Aydın S, Duman S et al. Growth and characterization of Ag/n-ZnO/p-Si/Al heterojunction diode by sol-gel spin technique. Journal of Alloys and Compounds 2013; 550: 129-132;Available from: https://doi.org/10.1016/j.jallcom.2012.09.131.
5. Oh D, No YS, Kim SY, Cho WJ, Kwack KD, Kim TW. Effect of Ag film thickness on the optical and the electrical properties in CuAlO2/Ag/CuAlO2 multilayer films grown on glass substrates. Journal of Alloys and Compounds 2011; 509: 2176-2179;Available from: https://doi.org/10.1016/j.jallcom.2010.10.180.
6. Zhang N, Xue F, Yu X, Zhou H, Ding E. Metal Fe3+ ions assisted synthesis of highly monodisperse Ag/SiO2 nanohybrids and their antibacterial activity. Journal of Alloys and Compounds 2013; 550: 209-215;Available from: https://doi.org/10.1016/j.jallcom.2012.09.090.
7. Kudelski A, Pisarek M, Roguska A, Hołdyński M, Janik-Czachor M. Surface-enhanced Raman scattering investigations on silver nanoparticles deposited on alumina and titania nanotubes: influence of the substrate material on surface-enhanced Raman scattering activity of Ag nanoparticles. Journal of Raman Spectroscopy 2012; 43: 1360-1366;Available from: https://doi.org/10.1002/jrs.4075.
8. Phuong NTT, Hoang TX, Tran NLN, Phuc LG, Phung V-D, Ta HKT et al. Rapid and sensitive detection of Rhodamine B in food using the plasmonic silver nanocube-based sensor as SERS active substrate. Spectrochimica Acta Part A: Molecular and Biomolecular Spectroscopy 2021; 263: 120179;PMID: 34298280. Available from: https://doi.org/10.1016/j.saa.2021.120179.
9. Liang H, Yang H, Wang W, Li J, Xu H. High-Yield Uniform Synthesis and Microstructure-Determination of Rice-Shaped Silver Nanocrystals. J Am Chem Soc 2009; 131: 6068-6069;PMID: 19364112. Available from: https://doi.org/10.1021/ja9010207.
10. Parnklang T, Lertvachirapaiboon C, Pienpinijtham P, Wongravee K, Thammacharoen C, Ekgasit S. H2O2-triggered shape transformation of silver nanospheres to nanoprisms with controllable longitudinal LSPR wavelengths. RSC Adv 2013; 3: 12886-12894;Available from: https://doi.org/10.1039/c3ra41486h.
11. Zheng M, Gu M, Jin Y, Jin G. Optical properties of silver-dispersed PVP thin film. Materials Research Bulletin 2001; 36: 853-859;Available from: https://doi.org/10.1016/S0025-5408(01)00525-6.
12. Liang H, Wang W, Huang Y, Zhang S, Wei H, Xu H. Controlled Synthesis of Uniform Silver Nanospheres. J Phys Chem C 2010; 114: 7427-7431;Available from: https://doi.org/10.1021/jp9105713.
13. Pandey A, Shankar S, Shikha, Arora NK. Amylase-assisted green synthesis of silver nanocubes for antibacterial applications. Bioinspired, Biomimetic and Nanobiomaterials 2019; 8: 161-170;Available from: https://doi.org/10.1680/jbibn.17.00031.
14. Wiley BJ, Chen Y, McLellan JM, Xiong Y, Li Z-Y, Ginger D et al. Synthesis and Optical Properties of Silver Nanobars and Nanorice. Nano Lett 2007; 7: 1032-1036;PMID: 17343425. Available from: https://doi.org/10.1021/nl070214f.
15. Nghia NV, Truong NNK, Thong NM, Hung NP. Synthesis of Nanowire-Shaped Silver by Polyol Process of Sodium Chloride. International Journal of Materials and Chemistry 2012; 2: 75-78;Available from: https://doi.org/10.5923/j.ijmc.20120202.06.
16. Guo S, Dong S, Wang E. Rectangular Silver Nanorods: Controlled Preparation, Liquid−Liquid Interface Assembly, and Application in Surface-Enhanced Raman Scattering. Crystal Growth & Design 2009; 9: 372-377;Available from: https://doi.org/10.1021/cg800583h.
17. Tian Cui-Feng, You Hong-Jun, Fang Ji-Xiang. Three-dimensional noble-metal nanostructure: A new kind of substrate for sensitive, uniform, and reproducible surface-enhanced Raman scattering. Chinese Phys B 2014; 23: 087801;Available from: https://doi.org/10.1088/1674-1056/23/8/087801.
18. Yang J, Cheng Q, Takahashi A, Goubaeva F. Kinetic Properties of GABA ρ1 Homomeric Receptors Expressed in HEK293 Cells. Biophysical Journal 2006; 91: 2155-2162;PMID: 16798806. Available from: https://doi.org/10.1529/biophysj.106.085431.
19. Yu D, Yam VW-W. Controlled Synthesis of Monodisperse Silver Nanocubes in Water. J Am Chem Soc 2004; 126: 13200-13201;PMID: 15479055. Available from: https://doi.org/10.1021/ja046037r.
20. Evanoff Jr. DD, Chumanov G. Synthesis and Optical Properties of Silver Nanoparticles and Arrays. ChemPhysChem 2005; 6: 1221-1231;PMID: 15942971. Available from: https://doi.org/10.1002/cphc.200500113.
21. Yaqoob AA, Umar K, Ibrahim MNM. Silver nanoparticles: various methods of synthesis, size affecting factors and their potential applications-a review. Appl Nanosci 2020; 10: 1369-1378;Available from: https://doi.org/10.1007/s13204-020-01318-w.
22. Hu B, Wang S-B, Wang K, Zhang M, Yu S-H. Microwave-Assisted Rapid Facile "Green" Synthesis of Uniform Silver Nanoparticles: Self-Assembly into Multilayered Films and Their Optical Properties. J Phys Chem C 2008; 112: 11169-11174;Available from: https://doi.org/10.1021/jp801267j.
23. Banerjee P, Satapathy M, Mukhopahayay A, Das P. Leaf extract mediated green synthesis of silver nanoparticles from widely available Indian plants: synthesis, characterization, antimicrobial property and toxicity analysis. Bioresour Bioprocess 2014;

1: 3;Available from: https://doi.org/10.1186/s40643-014-0003-y.
24. Santhoshkumar S, Murugan E. Size controlled silver nanoparticles on β-cyclodextrin/graphitic carbon nitride: an excellent nanohybrid material for SERS and catalytic applications. Dalton Trans 2021; 50: 17988-18000;PMID: 34851335. Available from: https://doi.org/10.1039/D1DT02809J.
25. Singh J, Kumar V, Singh Jolly S, Kim K-H, Rawat M, Kukkar D et al. Biogenic synthesis of silver nanoparticles and its photocatalytic applications for removal of organic pollutants in water. Journal of Industrial and Engineering Chemistry 2019; 80: 247-257;Available from: https://doi.org/10.1016/j.jiec.2019.08.002.
26. Al-Shalalfeh MM, Onawole AT, Saleh TA, Al-Saadi AA. Spherical silver nanoparticles as substrates in surface-enhanced Raman spectroscopy for enhanced characterization of ketoconazole. Materials Science and Engineering: C 2017; 76: 356-364;PMID: 28482538. Available from: https://doi.org/10.1016/j.msec.2017.03.081.
27. Al-Shalalfeh MM, Saleh TA, Al-Saadi AA. Silver colloid and film substrates in surface-enhanced Raman scattering for 2-thiouracil detection. RSC Adv 2016; 6: 75282-75292;Available from: https://doi.org/10.1039/C6RA14832H.
28. Bao NTG, Trang TNQ, Phuong PT, Thu VTH. Toward Plasmon-Controlled Generation of the Activating Ag Hotspot Nanospheres for Quantitative SERS Analysis. VNUHCM Journal of Science and Technology Development 2023; 26: 3008-3016;.
29. Shuang Shen X, Zhong Wang G, Hong X, Zhu W. Nanospheres of silver nanoparticles : agglomeration, surface morphology control and application as SERS substrates. Physical Chemistry Chemical Physics 2009; 11: 7450-7454;PMID: 19690718. Available from: https://doi.org/10.1039/b904712c.
30. Ma H, Yin B, Wang S, Jiao Y, Pan W, Huang S et al. Synthesis of Silver and Gold Nanoparticles by a Novel Electrochemical Method. ChemPhysChem 2004; 5: 68-75;PMID: 14999845. Available from: https://doi.org/10.1002/cphc.200300900.
31. Eustis S, Krylova G, Eremenko A, Smirnova N, Schill AW, El-Sayed M. Growth and fragmentation of silver nanoparticles in their synthesis with a fs laser and CW light by photosensitization with benzophenone. Photochem Photobiol Sci 2005; 4: 154-159;PMID: 15616707. Available from: https://doi.org/10.1039/b411488d.
32. Merga G, Wilson R, Lynn G, Milosavljevic BH, Meisel D. Redox Catalysis on "Naked" Silver Nanoparticles. J Phys Chem C 2007; 111: 12220-12226;Available from: https://doi.org/10.1021/jp074257w.
33. Meng Y. A Sustainable Approach to Fabricating Ag Nanoparticles/PVA Hybrid Nanofiber and Its Catalytic Activity. Nanomaterials (Basel) 2015; 5: 1124-1135;PMID: 28347055. Available from: https://doi.org/10.3390/nano5021124.
34. Lin S, Hasi W-L-J, Lin X, Han S-Q-G-W, Lou X, Yang F et al. Rapid and sensitive SERS method for determination of Rhodamine B in chili powder with paper-based substrates. Analytical methods 2015; 7: 5289;Available from: https://doi.org/10.1039/C5AY00028A.
35. Zhang J, Li X, Sun X, Li Y. Surface enhanced Raman scattering effects of silver colloids with different shapes. The Journal of Physical Chemistry B 2005; 109: 12544-12548;PMID: 16852551. Available from: https://doi.org/10.1021/jp050471d.
36. Tanvi, Mahajan A, Bedi RK, Kumar S, Saxena V, Singh A et al. Broadband enhancement in absorption cross-section of N719 dye using different anisotropic shaped single crystalline silver nanoparticles. RSC Adv 2016; 6: 48064-48071;Available from: https://doi.org/10.1039/C6RA08893G.
37. Cobley CM, Rycenga M, Zhou F, Li Z-Y, Xia Y. Controlled Etching as a Route to High Quality Silver Nanospheres for Optical Studies. J Phys Chem C 2009; 113: 16975-16982;Available from: https://doi.org/10.1021/jp906457f.
38. Cobley CM, Rycenga M, Zhou F, Li Z-Y, Xia Y. Etching and Growth: An Intertwined Pathway to Silver Nanocrystals with Exotic Shapes. Angewandte Chemie International Edition 2009; 48: 4824-4827;PMID: 19479923. Available from: https://doi.org/10.1002/anie.200901447.
39. Parnklang T, Lertvachirapaiboon C, Pienpinijtham P, Wongravee K, Thammacharoen C, Ekgasit S. H2O2-triggered shape transformation of silver nanospheres to nanoprisms with controllable longitudinal LSPR wavelengths. RSC Adv 2013; 3: 12886-12894;Available from: https://doi.org/10.1039/c3ra41486h.
40. Sarma TK, Chattopadhyay A. Starch-Mediated Shape-Selective Synthesis of Au Nanoparticles with Tunable Longitudinal Plasmon Resonance. Langmuir 2004; 20: 3520-3524;PMID: 15875377. Available from: https://doi.org/10.1021/la049970g.
41. Liu X, Xu H, Xia H, Wang D. Rapid Seeded Growth of Monodisperse, Quasi-Spherical, Citrate-Stabilized Gold Nanoparticles via H2O2 Reduction. Langmuir 2012; 28: 13720-13726;PMID: 22954316. Available from: https://doi.org/10.1021/la3027804.